Published in final edited form as:
J Immunol. 2009 May 1; 182(9): 5537–5546. doi:10.4049/jimmunol.0803742.

An Anti-Vascular Endothelial Growth Factor Receptor 2/Fetal Liver Kinase-1 *Listeria monocytogenes* Anti-Angiogenesis Cancer Vaccine for the Treatment of Primary and Metastatic Her-2/neu$^+$ Breast Tumors in a Mouse Model[1]

Matthew M. Seavey, **Paulo C. Maciag**[2], **Nada Al-Rawi**[3], **Duane Sewell**[4], and **Yvonne Paterson**[5]
Department of Microbiology, University of Pennsylvania School of Medicine, Philadelphia, PA 19104

Abstract

Thirty years after angiogenesis was shown to play an enabling role in cancer, modern medicine is still trying to develop novel compounds and therapeutics to target the tumor vasculature. However, most therapeutics require multiple rounds of administration and can have toxic side effects. In this study, we use anti-angiogenesis immunotherapy to target cells actively involved in forming new blood vessels that support the growth and spread of breast cancer. Targeting a central cell type involved in angiogenesis, endothelial cells, we immunized against host vascular endothelial growth factor receptor 2 to fight the growth of Her-2/neu$^+$ breast tumors. Using the bacterial vector, *Listeria monocytogenes* (*Lm*), we fused polypeptides from the mouse vascular endothelial growth factor receptor 2 molecule (fetal liver kinase-1) to the microbial adjuvant, listeriolysin-O, and used *Lm* to deliver the Ags and elicit potent antitumor CTL responses. *Lm*-listeriolysin-O-fetal liver kinase-1 was able to eradicate some established breast tumors, reduce microvascular density in the remaining tumors, protect against tumor rechallenge and experimental metastases, and induce epitope spreading to various regions of the tumor-associated Ag Her-2/neu. Tumor eradication was found to be dependent on epitope spreading to HER-2/neu and was not solely due to the reduction of tumor vasculature. However, vaccine efficacy did not affect normal wound healing nor have toxic side effects on pregnancy. We show that an anti-angiogenesis vaccine can overcome tolerance to the host vasculature driving epitope spreading to an endogenous tumor protein and drive active tumor regression.

Targeting host vasculature in an attempt to target chemoresistant tumors has been a central paradigm and a sought-after therapy in oncology for decades (1). First presented by Folkman (2), anti-angiogenic treatment has recently entered the clinic with the successful use of

[1]This work was supported by Grant 5RO1CA109253-03. M.M.S. and N.A.-R. were supported by Training Grant T32CA09140, “The Immunobiology of Normal and Neoplastic Lymphocytes.”

5 Address correspondence and reprint requests to Dr. Yvonne Paterson, Department of Microbiology, 323 Johnson Pavilion, 36th Street and Hamilton Walk, University of Pennsylvania School of Medicine, Philadelphia, PA 19104-6076. yvonne@mail.med.upenn.edu.
[2]Current address: Advaxis, North Brunswick, NJ 08902.
[3]Current address: Department of Pediatrics, Women and Infants Hospital of Rhode Island, Warren Alpert Medical School of Brown University, 101 Dudley Street, Providence, RI 02905.
[4]Current address: University of Maryland, 16 South Eutaw Street, Suite 500, Baltimore, MD 21201.

Disclosures
Yvonne Paterson and Paulo Cesar Maciag wish to disclose that they have a financial interest in Advaxis, a vaccine and therapeutic company that has licensed or has an option to license all patents from the University of Pennsylvania that concern the use of *Listeria monocytogenes* or listerial products as vaccines.

bevacizumab in several cancer types, including breast cancer (3). Since then, anti-angiogenesis treatments for cancer have multiplied, and several products are either in clinical use or trials (4).

Targeting cells involved in angiogenesis cripples rapidly growing tumors by limiting the oxygen and nutrients supply or, depending on the strategy used, increasing the susceptibility of tumor cells to chemotherapy by enhancing the efficiency of a delivered drug via vascular network reorganization (5,6). Although originally thought to be unlikely, resistance of tumor cells to anti-angiogenesis treatment has been observed in mouse systems and reported for human studies for several different treatments (7). Additionally, the tumor microenvironment recruits myeloid-derived suppressor cells that are responsible for the necessary angiogenic switch needed for tumor growth and eventual dissemination (8).

Studies performed by several investigators have repeatedly shown the importance of targeting tumor angiogenesis because of its central role in invasion, growth, and metastasis (9,10). Because tumor cells frequently mutate in response to therapy or down-regulate MHC class I molecules required for T cell-mediated responses, targeting endothelial cells and pericytes, which are essential for tumor survival and may lack the immunosuppressive mechanisms deployed by tumors, would be advantageous. Previously, we have shown that targeting pericytes in breast tumors, using an immunotherapy against the chondroitin sulfate molecule, high m.w. melanoma-associated Ag, results in lower pericyte coverage of tumor blood vessels, which leads to tumor cell death (11). In this study, we use the potent, live vaccine vector, *Listeria monocytogenes* (*Lm*),[6] to overcome tolerance to mouse fetal liver kinase-1 (Flk-1)/vascular endothelial growth factor (VEGF) receptor 2 (VEGFR2) and, indirectly, to Her-2/neu.

VEGFR2 is thought to be expressed on the luminal surface of activated or proliferating endothelial cells and participates in the formation of new blood vessels (12). It is the first endothelial receptor known to be expressed on the primitive mesoderm (13). VEGFR2 is highly expressed on endothelial cells (14). Strong induction of VEGFR2 is involved in the neovascularization of various human or experimental tumors (15). VEGFR2 binds all five isoforms of VEGF. Signaling of VEGF through VEGFR2 on endothelial cells induces proliferation, migration, and eventual differentiation. The mouse homologue of VEGFR2 is Flk-1, which is a strong therapeutic target (16,17), and has important roles in tumor growth, invasion, and metastasis (18,19). Several approaches have been used to block Flk-1, including dominant-negative receptor mutants, germline disruption of VEGFR genes, mAbs against VEGF, and a series of synthetic receptor tyrosine kinase inhibitors (20,21). Immunotherapeutic strategies have included targeting VEGFR2 using DNA vaccines delivered orally by *Salmonella typhimurium* (16). We have attempted to modify this approach by expressing three fragments of the VEGFR2 molecule fused to the microbial adjuvant listeriolysin-O (LLO) and expressed in *Lm.*

Lm is a Gram-positive facultative intracellular bacterium able to infect phagocytic cells (22) and whose life cycle makes it a valuable delivery vehicle for foreign proteins. After phagocytosis, *Lm* escapes the phagosome via the hemolytic virulence factor LLO, encoded by the *hly* gene, to replicate in the cytoplasm. Routinely, we engineer *Lm* to express our gene of interest fused to the first 441 aa so as to exclude the hemolytic domain of this protein (22-24). LLO contains a proline, glutamine acid, serine, threonine-rich (PEST) domain that is important for the adjuvant activity in the fused proteins (25).

[6]Abbreviations used in this paper: *Lm*, *Listeria monocytogenes*; DAPI, 4′,6′-diamidino-2-phenylindole; Flk-1, fetal liver kinase-1; HIF-1α, hypoxia-inducible factor-1α; LLO, listeriolysin-O; MVD, microvascular density; PEST, proline, glutamine acid, serine, threonine-rich; TIL, tumor-infiltrating lymphocyte; VEGF, vascular endothelial growth factor.

The use of *Lm* as a vaccine vector has shown promise for several different diseases (26). Our laboratory (23,24,27,28), as well as others (29-31), has repeatedly shown that *Listeria* can efficiently immunize mice against tumor proteins and overcome self-tolerance, and that it is safe for use in humans (32) (J. Rothman, unpublished clinical data). We show in this study that immunizing against the breast tumor vasculature leads to epitope spreading and immunity to Her-2/neu, which is required for tumor regression. Unlike several previous reports that also used VEGFR2 immunotherapy to target the tumor vasculature, in this study we describe a novel method of targeting both the tumor vasculature and an endogenous tumor Ag (Her-2/neu) using a single vaccine.

Materials and Methods

Mice

Female FVB/N mice were purchased from Charles River Laboratories. The FVB/N Her-2/neu transgenic mice were housed and bred at the animal core facility at the University of Pennsylvania. Mice were 6 – 8 wk old when used at the start of the experiments, which were done in accordance with regulations by the Institutional Animal Care and Use Committee of the University of Pennsylvania.

Peptides and Abs

Anti-mouse CD31, anti-mouse CD8α PE, and rat IgG2a PE isotype controls were purchased from BD Biosciences. Rabbit anti-*Listeria* antiserum polyclonal Ab, serotypes 1 and 4, was purchased from Difco BD Biosciences. Rabbit anti-hypoxia-inducible factor-1α (HIF-1α) was purchased from Novus Biologicals. Goat anti-rabbit Alexa-488 secondary Ab was purchased from Invitrogen. The 4′,6′-diamidino-2-phenylindole (DAPI) was purchased from Sigma-Aldrich. Rat anti-mouse IFN-γ (clone AN18) was purchased from Mabtech. Rat anti-mouse IFN-γ (clone XMG1.2) was purchased from eBioscience. The Abs used in the Western blot for fusion protein expression were either a polyclonal rabbit serum raised to the first 30 residues (PEST) of LLO protein (25) or an anti-LLO mouse Ab, specific for full-length LLO, generated from hybridoma supernatant, clone B5-19 (33). All peptides were purchased from EZBiolabs. Tetramers were provided by A. Stout (National Institutes of Health AIDS Research and Reference Reagent Program, Atlanta, GA). Tetramers used were all PE-conjugated H-2D^q and contained either peptides for Her-2/neu region EC1 (ASPETHLDML), EC2 (PDSLRDLSVF), or IC1 (GS GAFGTVYK). Peptides used in these studies were as follows: Flk-E1$_{210–219}$ (TYQSIMYIV), Flk-E2$_{613–622}$ (MFSNSTNDI), Flk-I1$_{906–915}$ (PGGPLM VIV), Flk-I1$_{839–848}$ (GRGAFGQVI) (17); Her2-pEC1$_{302–310}$ (PYNYL STEV), Her2-pEC2$_{420–429}$ (PDSLRDLSVF), Her2-pIC1$_{732–741}$ (GSGAF GTVYK) (24); and HIV-pGag (AMQMLKETI) (34).

ELISPOTs

Secretion of IFN-γ by mouse splenocytes in response to peptide stimulation was tested by ELISPOT assay, as previously described (29). We preferred to use ELISPOTs over other assays because of the level of sensitivity that could be obtained for low frequency, Ag-specific cells, and also because we could test for anti-Her-2/neu- and anti-Flk-1-specific T cells directly ex vivo without in vitro manipulation. Briefly, isolated splenocytes were plated at 1 × 10^6 cells/well or titrated across a 96-well plate coated with 7 μg/ml rat anti-mouse IFN-γ Ab (clone AN18; Mabtech), in the presence of 10 μg/ml peptide and 5 U/ml IL-2. Secondary, biotinylated, anti-IFN-γ Ab (clone XMG1.2; eBioscience) was added to each well at a final concentration of 2 μg/ml. After overnight incubation at 37°C, plates were developed for1hat room temperature with streptavidin-HRP (1/1000 dilution), followed by substrate tetramethylbenzidine (Vector Laboratories; ABC kit). Spots were counted using the Immunospot C.T.L. scanner and counting software (CTL).

Cell lines

Cell culture medium and supplements were purchased from Life Technologies (Invitrogen). NT-2 and J774A.1 cells were maintained, as previously described (11). All cell cultures were kept at 37°C and 5% CO_2. The 4T1 and 4T1 cells stably expressing the firefly luciferase gene (4T1-Luc) were the gift of E. Pure (Wistar Institute, Philadelphia, PA) and were maintained in cell culture medium.

Construction of Lm-*LLO-Flk-1 vaccines*

The source of the Flk-1 gene was a DNA vaccine plasmid provided by R. Reisfeld (Scripps Research Institute, La Jolla, CA). Fragments corresponding to residues 68–1081 were amplified by PCR using the following primers: Flk-E1 (F), 5′-GGGCTCGAGCGTGATTCTGAGGAAAGGGTATT-3′; Flk-E1 (R), 5′-GGGACTAGT**TTA**CCCGGTTTACAATCTTCTTA T-3′ (AA 68–277); Flk-E2 (F), 5′-GGGCTCGAGGTGATCAGGGGTCCTGAAATTA-3′; Flk-E2 (R), 5′-GGGACTAGT**TTA**GCCTCCATCCTCCTTCCT-3′ (aa 545–730); Flk-I1 (F), 5′-GGGCTCGAGGAAGGGGAACTGAAGACAGCC-3′; and Flk-I1 (R), 5′-GGGACTAGT**TTA**TGTGTATACTCTGTCAAAAATGGTTTC-3′ (aa 792-1081). *Xho*I sequence underlined for forward (F) primer, and *Spe*I sequence underlined for reverse (R) primer, with stop codon in bold. The PCR product was ligated into pCR2.1-TOPO plasmid (Invitrogen), confirmed by sequencing, and subsequently excised by double digestion with *Xho*I and *Spe*I (New England Biolabs). The fragment was ligated into a pGG34-based plasmid downstream and fused to a gene encoding for the first 441 residues of the LLO protein, whose expression is driven by the *hly* promoter. The construction of the pGG34 plasmid has been described in detail elsewhere (28). The resultant plasmid was electroporated into the PrfA-defective *Lm* strain XFL-7, which is derived from the *Lm* strain 10403S. Positive clones were selected on brain heart infusion (Difco) plates supplemented with 34 μg/ml chloramphenicol and 250 μg/ml streptomycin. The resultant stains were named *Lm*-LLO-Flk-E1, *Lm*-LLO-Flk-E2, and *Lm*-LLO-Flk-I1.

Growth and preparation of Lm *vaccine doses*

Vaccine stocks were kept at −80°C in 10% glycerol in 1× PBS. Each stock was streaked over a chloramphenicol/streptomycin plate and grown overnight. A single colony was used for growth in an overnight culture of 5 ml of brain heart infusion medium under antibiotic selection. This culture was further expanded for 4 h in a shaking incubator at 37°C and grown until the microbial density reached 0.4–0.8 OD_{600}, at which time the microbes were washed, frozen sterile in 10% glycerol, and kept at −80°C until use. Stocks were titered for each lot generated. Single lots were used for one continuous experiment, different lots were used for each repetition, and lot-to-lot variation was not observed. Each lot was checked for fusion protein expression by Western blot with an anti-PEST and anti-LLO Ab. For each dose, one vial is selected, thawed, and washed twice in 1× PBS before dilution and use; unused microbes are discarded.

Effect of Lm-*LLO-Flk-1 vaccines on tumor growth*

A total of 1×10^6 of NT-2 tumor cells was injected s.c. in 200 μl of PBS on the flank of FVB/N mice. On day 4 after tumor inoculation, mice were immunized i.p. with 5×10^8 CFUs of either *Lm*-LLO-Flk-E1, *Lm*-LLO-Flk-E2, or *Lm*-LLO-Flk-I1. This dose was determined as one-tenth of the minimum dose observed to have adverse effects on the mice, and was used in all experiments. Immunizations were repeated weekly, totaling three doses of the vaccine for all experiments. In the control groups, mice received a control *Lm* vaccine, *Lm*-LLO-NY-ESO-$1_{101–156}$. *Lm*-LLO-NY-ESO-$1_{101–156}$ acts as an irrelevant or third-party *Lm* vaccine to control for immune responses to LLO or the listerial infection; we commonly use this vaccine

as a control at comparable concentrations to the test vaccine (35). Tumors were measured every 3 days with calipers, and the shortest (width) and longest surface diameters were recorded for each individual tumor. Mice in groups were not blinded for tumor size. Calculated tumor volumes were performed using the following equation: $(\text{width}^2) \times \text{length} \times 0.52$. Mice were sacrificed if they developed open wounds or tumors reached 20 mm in diameter. Tumor-free surviving mice challenged with NT-2 were rechallenged in the opposite flank with the same cell line at least 10 wk after the first inoculation.

Tumor immunofluorescence

On day 64 posttumor inoculation, mice were sacrificed and the NT-2 tumors were surgically excised, cryopreserved in OCT freezing medium, and cryosectioned to provide 8- to 10-mm thick sections. For immunofluorescence, samples were thawed and fixed using 4% formalin. After blocking (2.4G2 conditioned medium/10% FBS/5% normal rat and mouse serum), sections were stained with primary Abs in blocking solution in a humidified chamber at 37°C for 1 h. Samples were stained with secondary Ab following the same procedure as used for primary staining. DAPI (Invitrogen) staining was performed according to manufacturer's instructions. Intracellular staining for HIF-1α was done in PBS/0.1% Tween 20/1% BSA solution. Slides were coverslipped using mounting solution (Biomeda) with anti-fading agents, set for 24 h, and kept at 4°C until imaged using Spot Image Software (version 2006) and a BX51 series Olympus fluores-cent microscope. Images were merged using Spot Image Software, and quantitation was performed after a region of interest was gated using Image Pro Software (version 2006). All images are a merged series of three different channels captured for the same exposure time. For the quantitation of microvascular density (MVD) using anti-CD31, we based our analysis on previously published works using similar strategies for measuring MVD in mouse tumor models (36–38).

Metastasis studies and bioluminescent imaging

Mice were given a total of three vaccinations before i.v. injection, 7 days postfinal vaccination, with 50,000 4T1 cells expressing the integrated luciferase reporter gene (4T1-Luc). The corresponding substrate, D-luciferin, was injected i.p. at 5–10 mg/mouse in 200 μl of PBS before imaging. The mice were placed in the dark chamber of a Xenogen IVIS imaging system (X-100; Xenogen), under anesthesia following i.p. injection of ketamine (80 mg/kg)/xylazine (12 mg/kg) (Sigma-Aldrich). Photographic and luminescence images were captured with a charge-coupled device camera, and the luminescence intensity was quantitated using Living Image software (version 2.11) from Xenogen, according to the manufacturer's instructions. Longitudinal imaging was performed on a weekly basis until at least 4 wk posttumor inoculation. All mice were imaged for the same exposure and length of time. Images show normalized graphics. For the pathology study, the identical experiment was performed, except lung tissue was perfused, extracted, wax embedded, and stained with H&E before being counted (by hand) for tumors.

Pregnancy and wound-healing safety studies

Six- to 8-wk-old FVB/N female mice were immunized three consecutive times weekly with either a control *Lm* vaccine or *Lm*-LLO-Flk-1 vaccines. In the fourth week, safety studies were conducted. For pregnancy and fertility, five mice per group were allowed to mate with individually housed males. Coitus was monitored and confirmed by the presence of a vaginal plug. Time to gestation, pup weight at birth, and total litter size were measured. The wound-healing assay used in this study was done according to previously described methods (11,16). Briefly, mice were anesthetized, hair was removed, and skin was cleaned with an aseptic wipe. Two circular, 3-mm-diameter wounds were punched from the skin using a sterile skin biopsy tool (Acuderm). Wounds were not treated, and no infection was observed. Average time to

wound closure was monitored and considered complete when a scar was formed without any visible scab left.

Statistical analysis and methods of quantitation

Data were analyzed using the nonparametric Mann-Whitney *U* test. The log-rank χ^2 test was used for all survival data. All statistical analysis was done with Prism software, version 4.0a (2006). Statistical significance was based on a value of $p \leq 0.05$. In all nontransgenic studies, we included at least eight mice per group. All studies were repeated at least once.

Results

A total of three constructs was tested, each containing a different region of Flk-1, as follows: E1 (aa 68–277), E2 (aa 545–730), and I1 (aa 792-1081) (Fig. 1*A*). Regions were selected based on predicted epitopes. Because we were interested in testing these vaccines in the FVB/N-based breast cancer model, we decided to clone fragments that would be most appropriate for the model haplotype used for testing (i.e., FVB/N, H-2^q). The E1, E2, and I1 domains selected contained several potential epitopes for the H-2^q mouse MHC I haplotype (Fig. 1*A*; Flk_{210} (TYQSIMYIV), Flk_{613} (MFSNSTNDI), and Flk_{906} (PGGPLMVIV)) (17,24).

Each fragment was cloned as a fusion protein with the truncated LLO protein (Fig. 1*B*). To test whether the LLO-Flk-1 fusion proteins were produced and secreted by the *Lm*-LLO-Flk-1 constructs, we analyzed protein from culture supernatants by Western blot (Fig. 1*C*) using a polyclonal anti-PEST Ab (Fig. 1*C*, *bottom*) or anti-LLO Ab (Fig. 1*C*, *top*). A band for each fusion construct was detected, LLO-Flk-E1, LLO-Flk-E2, and LLO-Flk-I1, each calculated from amino acid molecular mass to be ~81, 78, and 89 kDa, respectively. Several of the bands do not correlate exactly with the calculated molecular size; however, this is common and has been observed for other, similar vaccine constructs (24). The band ~60–70 kDa is endogenous LLO; the truncated fusion protein LLO is found at ~60–50 kDa (39). The anti-LLO blot was used as a control to show that our fusion proteins are LLO-Flk linked. All three constructs were able to infect, grow, and escape the phagolysosome, as evidenced by replication in J774A.1 macrophages (Fig. S1).[7] Also, each vaccine was able to immunize mice against cloned Flk-1 regions, as shown by IFN-γ splenocyte responses ex vivo (Fig. 1*D*). Peptides used for rechallenge in these FVB/N ELISPOT experiments were originally mapped in the H-2^d BALB/c mouse as immunodominant Flk-1 epitopes (17). We routinely use H-2^d-mapped epitopes in H-2^q models because H-2^d-identified epitopes can also serve as H-2^q epitopes (39–41), presumably due to the high homology of the H-2^d and H-2^q molecules (42).

Therapeutic efficacy of Lm-LLO-Flk-1 vaccines in a Her-2/neu-expressing tumor model

To test the ability of our vaccines to induce the regression of Her-2/neu^+ breast tumors, we used the NT-2 tumor model, which over-expresses the rat Her-2/neu as a transgene and was originally derived from a spontaneous mammary tumor in the FVB/N Her-2/ neu transgenic mouse (43). The NT-2 cell line does not express the Flk-1 molecule (44), and thus, our Ag of interest is only located on the host vasculature. Cells were grown in vitro and transplanted s.c. into the flank of FVB/N mice. On day 4, when palpable (~4–5 mm in diameter) tumors had formed, mice were vaccinated and then boosted weekly for a total of three vaccinations. Vaccines Flk-E1 and Flk-I1 were able to induce regression, and in some mice complete eradication (Flk-E1, 2 of 8; Flk-I1, 2 of 8) of transplanted tumors by day 64 postinoculation (Fig. 2*A*). However, Flk-E2 was unable to control tumor growth, which was similar to the group treated with the control *Lm*. Mice with completely regressed tumors were rechallenged with

[7]The online version of this article contains supplemental material.

NT-2 on the contralateral side at 100 days posttumor inoculation, and regrowth of the new tumor was not observed, suggesting long-lived antitumor immunity (Fig. 2, *C* and *D*).

MVD of day 64 tumors was assessed by staining with the panendothelial cell marker CD31 and counterstained with the nuclear marker DAPI. As expected, MVD in tumors from the Flk-E2-treated group resembled those from control-treated mice. However, a reduction in the density of $CD31^+$ vessels was seen in Flk-I1-treated mice, and a further reduction was observed using the Flk-E1 vaccination (Fig. 2*E*). This reduction in $CD31^+$ vessels correlated with an increase in staining for the nuclear hypoxic marker, HIF-1α, in the Flk-E1- and Flk-I1-treated groups, but not for the control group (data not shown). It is possible to hypothesize that regression of these Her-2/neu^+ tumors, in addition to the reduction of tumor MVD, was due to anti-VEGFR2 CTLs killing endothelial cells involved in tumor angiogenesis, possibly leading to tumor damage or growth restriction, resulting in the observed regression. Subsequently, phagocytosed tumor debris could be cross-presented by local dendritic cells in draining lymph nodes and presented to anti-Her-2/neu CTLs, whose epitopes have been previously mapped in the FVB/N mouse (24,39–41). If this intermolecular epitope spreading occurred, we would expect that mice that exhibited the greatest regression would also have a high frequency of anti-Her-2/neu $CD8^+$ T cells. To test this hypothesis, we harvested splenocytes from day 64 mice, and performed an IFN-γ ELISPOT, rechallenging with three known epitopes from three different regions of Her-2/neu (24). We decided to use an ELISPOT assay to measure anti-Her-2/neu responses because we had previously mapped CTL epitopes for different regions of the Her-2/neu molecule and the ELISPOT assay is sensitive enough to detect a low frequency of specific T cells, unlike several cytotoxic assays that require in vitro stimulation and expansion. We found that Flk-E1 and Flk-I1 showed the greatest epitope spreading, whereas Flk-E2 showed the least (Fig. 2*B*; *, $p < 0.05$), strongly correlating with the extent of tumor regression found in vivo (Fig. 2*A*).

Anti-angiogenesis-induced tumor regression is dependent on epitope spreading to an endogenous tumor Ag

The presence of Her-2/neu epitope spreading suggested that tumor regression may not solely depend on antivascular events, but also on the immune response to the tumor Ag HER-2/neu. To test this hypothesis, we repeated the same experiment using the two most potent vaccines, Flk-E1 and Flk-I1, but, in addition to inoculation of wild-type FVB/N mice, we also injected the NT-2 cells s.c. into its syngeneic progenitor strain, FVB/N Her-2/neu transgenic, which exhibits profound tolerance to the rat Her-2/neu molecule (41,43). Again, Flk-E1 and Flk-I1 slowed the growth of the NT-2 tumors in wild-type FVB/N mice, as previously demonstrated (Fig. 3*A*, *left panel*); however, in the transgenic host in which anti-HER-2/neu responses are limited by tolerance, we observed outgrowth of all tumors (Fig. 3*A*, *right panel*). Both of these results reflected the epitope spreading observed toward the endogenous Her-2/neu protein demonstrated in the spleen (Fig. 3*B*) and at the tumor site, as shown for the Flk-E1 vaccination (Fig. 3*C*). This suggests that antivascular events are not enough for tumor regression, but rather, the combined effect on both the tumor's vasculature and directly on tumor cells is required for tumor death and ultimately regression.

Vaccination with Lm-LLO-Flk-1 vaccine fragments can prevent the growth of experimental metastases

An important use for anti-angiogenesis vaccines could be for the treatment or prevention of breast cancer metastasis. Tumor cells that metastasize are highly dependent on the development of new vessels, although smaller tumors do not completely rely on new vasculature (45). However, it has been hypothesized that once they have grown beyond a certain size, tumors become highly dependent on the formation of new vessels (46), and thus become a possible target for anti-VEGFR2 CTLs. To test whether our vaccines could protect against breast tumor

dissemination, we used an experimental metastasis system involving the direct inoculation of in vitro cultured tumor cells into the tail vein of mice, allowing for rapid colonization of several downstream organs, especially the lung (47). Because after tail vein vaccination the NT-2 model does not well colonize the lung (data not shown), we used 4T1, which is an aggressive, mouse breast carcinoma cell line from the BALB/c mouse. BALB/c mice were immunized thrice over the course of 3 wk with either *Lm*-LLO-Flk-E1, *Lm*-LLO-Flk-I1, or a control *Lm* vaccine. Mice were then injected with 50,000 4T1 cells i.v. and also s.c. within the same animal. The s.c. site injection was performed so that we could measure primary tumor growth, whereas the i.v. injection mimicked metastasis. Mice treated with the Flk-1 vaccines had reduced primary s.c. tumor growth rate (Fig. 4*D*). Unlike the poor responses seen against the primary 4T1 tumor, the rate of seeding and total metastases found in each animal was significantly lower in treated animals compared with control-treated mice (Fig. 4*A*). We observed a low level of epitope spreading to Her-2/neu (Fig. 4*B*), probably because 4T1 weakly expresses the mouse Her-2/neu (48).

To more stringently test the hypothesis that immunizing against Flk-1 can prevent the seeding of lung tissue with experimental metastases, we used a bioluminescent model in which individual tumor cells and masses can be visualized using noninvasive imaging. Mice were injected i.v. with 50,000 4T1 cells expressing the firefly luciferase gene (4T1-Luc) after several rounds of vaccination with the *Lm*-Flk-E1 and *Lm*-Flk-I1 vaccines. On a weekly basis, mice were anesthetized and injected with a luciferase substrate (D-luciferin) and imaged. Lung seeding was apparent by day 11, and control-treated mice rapidly become colonized with 4T1-Luc cells by day 25, whereas none of the *Lm*-LLO-Flk-E1- and *Lm*-LLO-Flk-I1-treated mice showed any signs of lung seeding until at least day 32, at which point the control-treated mice had become ill and were sacrificed (Fig. 4*C*). At day 32, only 25% of the Flk-1-vaccinated mice showed any lung tumors. It is possible that tumor masses were undetectable at this time point by this bioluminescent method because a signal for tumor cells was observed on day 25, but not day 32 for the *Lm*-Flk-E1-treated group. This very small signal on day 25 is below the 1000 cell threshold and may have lost some cellular mass within the following week to fall below the limit of detection for the system. Mice immunized with the control *Lm* rapidly became diseased by lung tumors, but the Flk-E1 and Flk-I1 *Lm* vaccinations delayed tumor burden, time to progression (day 25 for control treated vs day 32 for Flk-1 treated), and eventual disease (data not shown).

Immunization with Flk-1 has no impact on wound healing, pregnancy, or fertility in mice

To evaluate whether *Lm*-LLO-Flk-1 vaccines cause toxicity that is associated with angiogenesis inhibition, we studied wound healing, pregnancy, and fertility in immunized mice. Mice were immunized thrice with *Lm*-LLO-Flk-E1, *Lm*-LLO-Flk-E2, *Lm*-LLOFlk-I1, control *Lm*, or saline alone before being mated or given sterile wound punches. We observed mice that were mated for length of gestation from coitus, mean pup mass at term, and total litter size. Wound punches were sterile, but mice were caged together. Wound-healing technique was followed according to previously described methods (16). Five mice from each immunization group were shaved and given sterile wound punches, two per animal, and then allowed to heal over time. Time to wound closure was measured. Full wound healing was considered complete; no scabs were left at time of wound closure. Immunization with *Lm*-LLO-Flk-E1, *Lm*-LLO-Flk-E2, or *Lm*-LLO-Flk-I1 had no impact on fertility, gestation length, or pup mass at birth (Fig. 5*A*). Similarly, immunization had no significant impact on the time required for wound closure (Fig. 5*B*).

Discussion

The advantage of using *Lm* to deliver a self protein fused to the microbial adjuvant LLO is that we are able to overcome tolerance to VEGFR2 on host endothelial cells as well as generate an immune response to the rat Her-2/neu endogenous tumor Ag found on transplanted tumor cells. Driving immune responses to a defined tumor Ag expressed by the tumor cells via the indirect targeting of the tumor vasculature is a novel finding, and warrants additional investigation for the manipulation and benefit of this vaccination strategy.

The Flk-E1 and Flk-I1 vaccinations were the most effective and could induce the greatest regression, MVD reduction, and epitope spreading in NT-2 tumor models. In contrast, although the Flk-E2 vaccination could generate strong immune responses in vivo against Flk Ags, it failed to induce the regression of NT-2, which led to poor epitope spreading and vascular destruction (Fig. 2). It is possible that the Flk-E2 vaccine is generating weakly cytotoxic CTLs; this has yet to be tested. The reduced vaccine efficacy of Flk-E2 is unlikely to be due to differences between the expression of the fusion protein by the vaccines because all three vaccines have similar expression levels (Fig. 1*B*). However, the presence of intact tumor vessels in Flk-E2-vaccinated mice (Fig. 2*E*) suggests that targets are being spared; thus, CTLs are either being generated at a very low frequency, or the cells that are being generated are of low avidity. Another possibility is that Flk-E2 could be inducing T regulatory cells, as has been shown for previous vaccines (23), which hinder cytolytic function of antitumor $CD8^+$ T cells in vivo.

Another possible reason for the poor performance of the Flk-E2 vaccine could be that Flk-E1 and Flk-I1 share regions of homology with Her-2/neu that Flk-E2 fragments do not. Her-2/neu is part of the epidermal growth factor receptor family, which is related to the VEGFR family (49). The overall protein homology between mouse Flk-1 and rat Her-2/neu is fairly low (5.37%); they primarily share sequence identity in the protein kinase signaling domain. Homology between Flk-E1 and rat Her-2/neu is nonexistent; thus, for this vaccine it seems highly unlikely that anti-Her-2/neu responses do not arise by epitope spreading. The greatest levels of homology between Flk-I1 and the kinase domains of Her-2/neu are 41% with a 168-aa-long stretch in rat Her-2/*neu*, aa 817–983, and 22% in a 200-aa-long stretch at aa 627–821, both that we have previously mapped for Her-2/neu and identified several CTL epitopes (41). Within these sequences we found similarities in Flk-1, with only two of the known Her-2/neu epitopes, as follows: the mouse Flk-1 sequence, KICDFGLARD (aa 1041–1050), is similar to the rat Her-2/neu epitope, KITDFGLARL(aa 861–870); and the mouse Flk-1 sequence, GRGAFGQVI (aa 839–848), is also similar to the rat Her-2/neu epitope, GSGAFGTVYK (aa 732–741). Missing homology is underlined; mutations that result after immunization with anti-Her-2/neu *Lm* vaccinations are in bold (39). However, a RANKpep analysis shows that the mouse Flk-$I1_{839–848}$ is the only likely epitope (http://mif.dfci.harvard.edu/Tools/rankpep.html; analysis not shown). We thus tested whether immunization of FVB/N mice with Flk-I1 vaccine could induce immunity to FLK-$I1_{839–848}$, which is cross-reactive to the rat Her-2/neu epitope GSGAFGTVYK. Vaccination of mice with *Lm*-LLO-Flk-I1 led to excellent responses against the previously mapped Flk-I1 epitope PGGPLMVIV (17); however, no signifi-cant responses were seen against either the mouse Flk-$I1_{839–848}$ epitope or the homologous rat Her-2/neu $IC1_{732–741}$ epitope (Fig. 6). Thus, the immune responses to Her-2/neu observed after Flk-I1 immunization were most likely due to epitope spreading and not due to cross-reactivity between shared epitopes. However, we cannot definitely say that cross-reactivity to Her-2/neu shared domains is not occurring; rather, the likelihood of this event seems very low.

The finding that an anti-angiogenesis vaccine induces secondary antitumor responses that are crucial to its efficacy is novel and opens the door for several possible vaccination strategies

that harness the power of this epitope-spreading phenomenon. To extend on this observation, an interesting possibility would be to boost the secondary anti-Her-2/neu response generated at an additional time point after therapy. We suspect that this would provide additional protection from residing tumor cells, or tumor stem cells, because Her-2/neu is also highly expressed on these cell types (50).

A difficulty encountered in targeting the vasculature of tumors is that when vessels are destroyed, current or additional therapy is unable to reach the tumor. Hypoxic areas of the tumor may become difficult to treat after anti-angiogenic therapy; however, tumors overexpress survival factors, mutate checkpoint proteins like p53, and constitutively express certain hypoxia-induced genes that allow tumors to become resistant to such conditions. The current theory of how anti-angiogenesis treatment functions is that tumor vessels become reorganized to a more normal infrastructure, allowing for the efficient delivery of treatment (6). However, the MVD loss observed in this study suggests that vessel integrity is nearly completely lost and is strongly associated with regressing tumors. However, it appears that tumor-specific tumor-infiltrating lymphocytes (TILs) can enter the tumor and remain in the tissue weeks postvaccination (Fig. 3*C*). Thus, disruption of the tumor vasculature either is not enough to reduce TIL trafficking or the influx of immune cells occurs before the disintegration of the tumor's vascular network.

It is perhaps surprising that the Flk-1 vaccine can mediate tumor vessel destruction without causing significant problems during pregnancy and wound healing (Fig. 5). However, angiogenesis during tumor development differs significantly from the highly organized, slow growth of wound healing or the uterine NK cell-driven angiogenesis and spiral artery formation seen during implantation and placenta development (51). We hypothesize that rapid vessel formation and unorganized and improper development of vascular networks associated with poor pericyte coverage in tumors increase the susceptibility of tumor tissue to anti-angiogenesis therapy. In addition, tissue specificity and cells involved in tumor vessel recruitment differ from superficial wounds, although many similarities still exist (52). For instance, the inflammatory environment for an invasive tumor is similar for cell types and cytokines involved in wound repair. However, the rate of new vessel growth and sheer numbers of trafficking leukocytes are greater for tumors (52).

Commercialized anti-angiogenesis immunotherapies have mainly been restricted to Abs binding either VEGF-A or VEGFRs; several nonimmunotherapies have targeted inhibiting the downstream function of key receptors (e.g., VEGFR1/2, platelet-derived growth factor receptor) such as Sorafenib (Nexavar). However, several experimental forms of anti-angiogenic immunotherapy are either in preclinical or clinical development. These include the use of whole fixed endothelial cells (53), VEGFR2-conjugated proteins (54), pulsed dendritic cells (55), liposomal peptide for fibro-blast growth factor-2 (56), and several DNA vaccines immunizing against survivin, integrin β_3, VEGF, VEGFR2 (see review (57)), and even live vaccine vectors used as shuttles for DNA vaccines against VEGFR2 and Endoglin/CD105 (16,58).

Using immunotherapy to target the vasculature presents several advantages over the passive administration of purified Abs, one being the ability to boost the initial immune response overtime and the cost of vaccination. However, presented in this study is the novel use of a recombinant fusion protein-expressing *Lm* vector, which presents several advantages over the use of other bacterial vectors. Our *Lm*-LLO-Flk-1 strains increase the immunogenicity of the Flk-1 fragment via fusion to LLO, are highly attenuated, and primarily replicate within macrophages and dendritic cells. Both the inflammatory response to infection with *Listeria* and the additional responses induced by our fusion protein constructs have the power to

simultaneously reduce T regulatory cell numbers at the site of the tumor while inducing potent antitumor CTLs (23).

Metastatic breast cancer is especially susceptible to anti-angiogenesis treatment because metastases need to recruit new vessels when becoming established at distant locations from the primary tumor site (45). Several clinical studies suggest that micrometastases can exist in a growth-static state at ~1–3 mm in diameter and feed from the passive movement of molecules. However, to support tumor growth beyond 3 mm, the new synthesis of a vascular network is required (46). It is at this point that we anticipate the maximum benefit from our anti-VEGFR2 vaccines, which may possibly blunt the spread of metastatic breast cancer.

Supplementary Material

Refer to Web version on PubMed Central for supplementary material.

Acknowledgments

We give a special thanks to Dr. Ellen Pure for the 4T1-Luc cells and Dr. Ralph Reisfeld for the original Flk-1 plasmid. The imaging data presented in this study were performed at the Optical Imaging Core of the Small Animal Imaging Facility at the University of Pennsylvania. We are also grateful to Dr. Yingqui Yvette Liu and Dr. Wafik S. El-Deiry for advice and assistance on the part of the optical imaging study.

References

1. Si ZC, Liu J. What “helps” tumors evade vascular targeting treatment? Chin. Med. J 2008;121:844–849. [PubMed: 18701052]
2. Folkman J. Tumor angiogenesis: therapeutic implications. N. Engl. J. Med 1971;285:1182–1186. [PubMed: 4938153]
3. Widakowich C, Dinh P, de Azambuja E, Awada A, Piccart-Gebhart M. HER-2 positive breast cancer: what else beyond trastuzumab-based therapy? Anticancer Agents Med. Chem 2008;8:488–496. [PubMed: 18537532]
4. Esteva FJ. Monoclonal antibodies, small molecules, and vaccines in the treatment of breast cancer. Oncologist 2004;9(Suppl 3):4–9. [PubMed: 15163841]
5. Hida K, Hida Y, Shindoh M. Understanding tumor endothelial cell abnormalities to develop ideal anti-angiogenic therapies. Cancer Sci 2008;99:459–466. [PubMed: 18167133]
6. Jain RK. Normalization of tumor vasculature: an emerging concept in antiangiogenic therapy. Science 2005;307:58–62. [PubMed: 15637262]
7. Bergers G, Hanahan D. Modes of resistance to anti-angiogenic therapy. Nat. Rev. Cancer 2008;8:592–603. [PubMed: 18650835]
8. Noonan DM, De Lerma Barbaro A, Vannini N, Mortara L, Albini A. Inflammation, inflammatory cells and angiogenesis: decisions and indecisions. Cancer Metastasis Rev 2008;27:31–40. [PubMed: 18087678]
9. Folkman J. Angiogenesis and angiogenesis inhibition: an overview. EXS 1997;79:1–8. [PubMed: 9002217]
10. Eberhard A, Kahlert S, Goede V, Hemmerlein B, Plate KH, Augustin HG. Heterogeneity of angiogenesis and blood vessel maturation in human tumors: implications for antiangiogenic tumor therapies. Cancer Res 2000;60:1388–1393. [PubMed: 10728704]
11. Maciag PC, Seavey MM, Pan Z-K, Ferrone S, Paterson Y. Cancer immunotherapy targeting the HMW-MAA protein results in a broad anti-tumor response and reduction of pericytes in the tumor vasculature. Cancer Res 2008;68:8066–8075. [PubMed: 18829565]
12. Shalaby F, Ho J, Stanford WL, Fischer KD, Schuh AC, Schwartz L, Bernstein A, Rossant J. A requirement for Flk1 in primitive and definitive hematopoiesis and vasculogenesis. Cell 1997;89:981–990. [PubMed: 9200616]

13. Yamaguchi TP, Dumont DJ, Conlon RA, Breitman ML, Rossant J. flk-1, an flt-related receptor tyrosine kinase is an early marker for endothelial cell precursors. Development 1993;118:489–498. [PubMed: 8223275]
14. Millauer B, Wizigmann-Voos S, Schnurch H, Martinez R, Moller NP, Risau W, Ullrich A. High affinity VEGF binding and developmental expression suggest Flk-1 as a major regulator of vasculogenesis and angiogenesis. Cell 1993;72:835–846. [PubMed: 7681362]
15. Millauer B, Longhi MP, Plate KH, Shawver LK, Risau W, Ullrich A, Strawn LM. Dominant-negative inhibition of Flk-1 suppresses the growth of many tumor types in vivo. Cancer Res 1996;56:1615–1620. [PubMed: 8603410]
16. Niethammer AG, Xiang R, Becker JC, Wodrich H, Pertl U, Karsten G, Eliceiri BP, Reisfeld RA. A DNA vaccine against VEGF receptor 2 prevents effective angiogenesis and inhibits tumor growth. Nat. Med 2002;8:1369–1375. [PubMed: 12415261]
17. Luo Y, Markowitz D, Xiang R, Zhou H, Reisfeld RA. FLK-1-based minigene vaccines induce T cell-mediated suppression of angiogenesis and tumor protective immunity in syngeneic BALB/c mice. Vaccine 2007;25:1409–1415. [PubMed: 17113202]
18. Folkman J. Tumor angiogenesis and tissue factor. Nat. Med 1996;2:167–168. [PubMed: 8574960]
19. Shibuya M. Vascular endothelial growth factor (VEGF)-receptor 2: its biological functions, major signaling pathway, and specific ligand VEGF-E. Endothelium 2006;13:63–69. [PubMed: 16728325]
20. Strawn LM, McMahon G, App H, Schreck R, Kuchler WR, Longhi MP, Hui TH, Tang C, Levitzki A, Gazit A, et al. Flk-1 as a target for tumor growth inhibition. Cancer Res 1996;56:3540–3545. [PubMed: 8758924]
21. Taraboletti G, Margosio B. Antiangiogenic and antivascular therapy for cancer. Curr. Opin. Pharmacol 2001;1:378–384. [PubMed: 11710736]
22. Seavey, MM.; Verch, T.; Paterson, Y. Anticancer vaccine strategies. In: Liu, D., editor. Handbook of Listeria monocytogenes. CRC Press, Taylor and Francis Group; Boca Raton, FL: 2008. p. 481-511.Ch. 16
23. Hussain SF, Paterson Y. What is needed for effective antitumor immunotherapy? Lessons learned using *Listeria monocytogenes* as a live vector for HPV-associated tumors. Cancer Immunol. Immunother 2005;54:577–586. [PubMed: 15650885]
24. Singh R, E. Dominiecki M, M. Jaffee E, Paterson Y. Fusion to listeriolysin O and delivery by *Listeria monocytogenes* enhances the immunogenicity of HER-2/*neu* and reveals subdominant epitopes in the FVB/N mouse. J. Immunol 2005;175:3663–3673. [PubMed: 16148111]
25. Sewell DA, Shahabi V, Gunn GR III, Pan Z-K, Dominiecki ME, Paterson Y. Recombinant *Listeria* vaccines containing PEST sequences are potent immune adjuvants for the tumor-associated antigen human papilloma-virus-16 E7. Cancer Res 2004;64:8821–8825. [PubMed: 15604239]
26. Bruhn KW, Craft N, Miller JF. *Listeria* as a vaccine vector. Microb. Infect 2007;9:1226–1235.
27. Pan Z-K, Weiskirch LM, Paterson Y. Regression of established B16F10 melanoma with a recombinant *Listeria monocytogenes* vaccine. Cancer Res 1999;59:5264–5269. [PubMed: 10537307]
28. Gunn GR, Zubair A, Peters C, Pan Z-K, Wu TC, Paterson Y. Two *Listeria monocytogenes* vaccine vectors that express different molecular forms of human papilloma virus-16 (HPV-16) E7 induce qualitatively different T cell immunity that correlates with their ability to induce regression of established tumors immortalized by HPV-16. J. Immunol 2001;167:6471–6479. [PubMed: 11714814]
29. Shahabi V, Reyes-Reyes M, Wallecha A, Rivera S, Paterson Y, Maciag P. Development of a *Listeria monocytogenes* based vaccine against prostate cancer. Cancer Immunol. Immunother 2008;57:1301–1313. [PubMed: 18273616]
30. Brockstedt DG, Giedlin MA, Leong ML, Bahjat KS, Gao Y, Luckett W, Liu W, Cook DN, Portnoy DA, Dubensky, Jr TW. *Listeria*-based cancer vaccines that segregate immunogenicity from toxicity. Proc. Natl. Acad. Sci. USA 2004;101:13832–13837. [PubMed: 15365184]
31. Bruhn KW, Craft N, Nguyen BD, Yip J, Miller JF. Characterization of anti-self CD8 T-cell responses stimulated by recombinant *Listeria monocytogenes* expressing the melanoma antigen TRP-2. Vaccine 2005;23:4263–4272. [PubMed: 15913853]

32. Brockstedt DG, Dubensky TW. Promises and challenges for the development of *Listeria monocytogenes*-based immunotherapies. Exp. Rev. Vaccines 2008;7:1069–1084.
33. Edelson BT, Unanue ER. Intracellular antibody neutralizes *Listeria* growth. Immunity 2001;14:503–512. [PubMed: 11371353]
34. Mata M, Yao ZJ, Zubair A, Syres K, Paterson Y. Evaluation of a recombinant *Listeria monocytogenes* expressing an HIV protein that protects mice against viral challenge. Vaccine 2001;19:1435–1445. [PubMed: 11163666]
35. Maciag PC, Seavey MM, Pan Z-K, Ferrone S, Paterson Y. Cancer immunotherapy targeting the high molecular weight melanoma-associated antigen protein results in a broad antitumor response and reduction of pericytes in the tumor vasculature. Cancer Res 2008;68:8066–8075. [PubMed: 18829565]
36. Yunmbam MK. Inhibition of breast cancer in nude mouse model by anti-angiogenesis. Oncol. Rep 1998;5:1431–1437. [PubMed: 9769382]
37. Shimizu M, Shimamura M, Owaki T, Asakawa M, Fujita K, Kudo M, Iwakura Y, Takeda Y, Luster AD, Mizuguchi J, Yoshimoto T. Antiangiogenic and antitumor activities of IL-27. J. Immunol 2006;176:7317–7324. [PubMed: 16751375]
38. Gyorffy S, Palmer K, Podor TJ, Hitt M, Gauldie J. Combined treatment of a murine breast cancer model with type 5 adenovirus vectors expressing murine angiostatin and IL-12: a role for combined anti-angiogenesis and immunotherapy. J. Immunol 2001;166:6212–6217. [PubMed: 11342643]
39. Singh R, Paterson Y. Immunoediting sculpts tumor epitopes during immunotherapy. Cancer Res 2007;67:1887–1892. [PubMed: 17332314]
40. Singh R, Paterson Y. Vaccination strategy determines the emergence and dominance of $CD8^+$ T-cell epitopes in a FVB/N rat HER-2/*neu* mouse model of breast cancer. Cancer Res 2006;66:7748–7757. [PubMed: 16885378]
41. Singh R, Paterson Y. In the FVB/N HER-2/*neu* transgenic mouse both peripheral and central tolerance limit the immune response targeting HER-2/*neu* induced by *Listeria monocytogenes*-based vaccines. Cancer Immunol. Immunother 2007;56:927–938. [PubMed: 17131121]
42. Rubocki RJ, Lee DR, Lie WR, Myers NB, Hansen TH. Molecular evidence that the H-2D and H-2L genes arose by duplication: differences between the evolution of the class I genes in mice and humans. J. Exp. Med 1990;171:2043–2061. [PubMed: 2351932]
43. Ercolini AM, Ladle BH, Manning EA, Pfannenstiel LW, Armstrong TD, Machiels JP, Bieler JG, Emens LA, Reilly RT, Jaffee EM. Recruitment of latent pools of high-avidity $CD8^+$ T cells to the antitumor immune response. J. Exp. Med 2005;201:1591–1602. [PubMed: 15883172]
44. Manning EA, Ullman JG, Leatherman JM, Asquith JM, Hansen TR, Armstrong TD, Hicklin DJ, Jaffee EM, Emens LA. A vascular endothelial growth factor receptor-2 inhibitor enhances antitumor immunity through an immune-based mechanism. Clin. Cancer Res 2007;13:3951–3959. [PubMed: 17606729]
45. Augustin HG. Antiangiogenic tumour therapy: will it work? Trends Pharmacol. Sci 1998;19:216–222. [PubMed: 9666712]
46. Heidenreich R, Kappel A, Breier G. Tumor endothelium-specific transgene expression directed by vascular endothelial growth factor receptor-2 (Flk-1) promoter/enhancer sequences. Cancer Res 2000;60:6142–6147. [PubMed: 11085538]
47. Pulaski, BA.; Ostrand-Rosenberg, S. Mouse 4T1 breast tumor model. In: Coligan, JE., editor. Current Protocols in Immunology. John Wiley and Sons, Inc.; New York, NY: 2001. p. 20.2.1-20.2.16.Ch. 20
48. Seavey MM, Pan Z-K, Maciag PC, Wallecha A, Rivera S, Paterson Y, Shahabi V. A novel human Her-2/*neu* chimeric molecule expressed by *Listeria monocytogenes* can elicit potent HLA-A2 restricted $CD8^+$ T cell responses and impact the growth and spread of Her-2/neu^+ breast tumors. Clin. Cancer Res 2009;15:924–932. [PubMed: 19188163]
49. Hatake K, Tokudome N, Ito Y. Next generation molecular targeted agents for breast cancer: focus on EGFR and VEGFR pathways. Breast Cancer 2007;14:132–149. [PubMed: 17485898]
50. Korkaya H, Paulson A, Iovino F, Wicha MS. HER2 regulates the mammary stem/progenitor cell population driving tumorigenesis and invasion. Oncogene 2008;27:6120–6130. [PubMed: 18591932]

51. Leonard S, Murrant C, Tayade C, van den Heuvel M, Watering R, Croy BA. Mechanisms regulating immune cell contributions to spiral artery modification: facts and hypotheses: a review. Placenta 2006;27(Suppl A):S40–S46. [PubMed: 16413937]
52. Schafer M, Werner S. Cancer as an overhealing wound: an old hypothesis revisited. Nat. Rev. Mol. Cell Biol 2008;9:628–638. [PubMed: 18628784]
53. Wei YQ, Wang QR, Zhao X, Yang L, Tian L, Lu Y, Kang B, Lu CJ, Huang MJ, Lou YY, et al. Immunotherapy of tumors with xenogeneic endothelial cells as a vaccine. Nat. Med 2000;6:1160–1166. [PubMed: 11017149]
54. Liu JY, Wei YQ, Yang L, Zhao X, Tian L, Hou JM, Niu T, Liu F, Jiang Y, Hu B, et al. Immunotherapy of tumors with vaccine based on quail homologous vascular endothelial growth factor receptor-2. Blood 2003;102:1815–1823. [PubMed: 12750177]
55. Li Y, Wang MN, Li H, King KD, Bassi R, Sun H, Santiago A, Hooper AT, Bohlen P, Hicklin DJ. Active immunization against the vascular endothelial growth factor receptor flk1 inhibits tumor angiogenesis and metastasis. J. Exp. Med 2002;195:1575–1584. [PubMed: 12070285]
56. Plum SM, Holaday JW, Ruiz A, Madsen JW, Fogler WE, Fortier AH. Administration of a liposomal FGF-2 peptide vaccine leads to abrogation of FGF-2-mediated angiogenesis and tumor development. Vaccine 2000;19:1294–1303. [PubMed: 11137269]
57. Okaji Y, Tsuno NH, Saito S, Yoneyama S, Tanaka M, Nagawa H, Takahashi K. Vaccines targeting tumor angiogenesis: a novel strategy for cancer immunotherapy. Eur. J. Surg. Oncol 2006;32:363–370. [PubMed: 16520018]
58. Lee SH, Mizutani N, Mizutani M, Luo Y, Zhou H, Kaplan C, Kim SW, Xiang R, Reisfeld RA. Endoglin (CD105) is a target for an oral DNA vaccine against breast cancer. Cancer Immunol. Immunother 2006;55:1565–1574. [PubMed: 16565828]

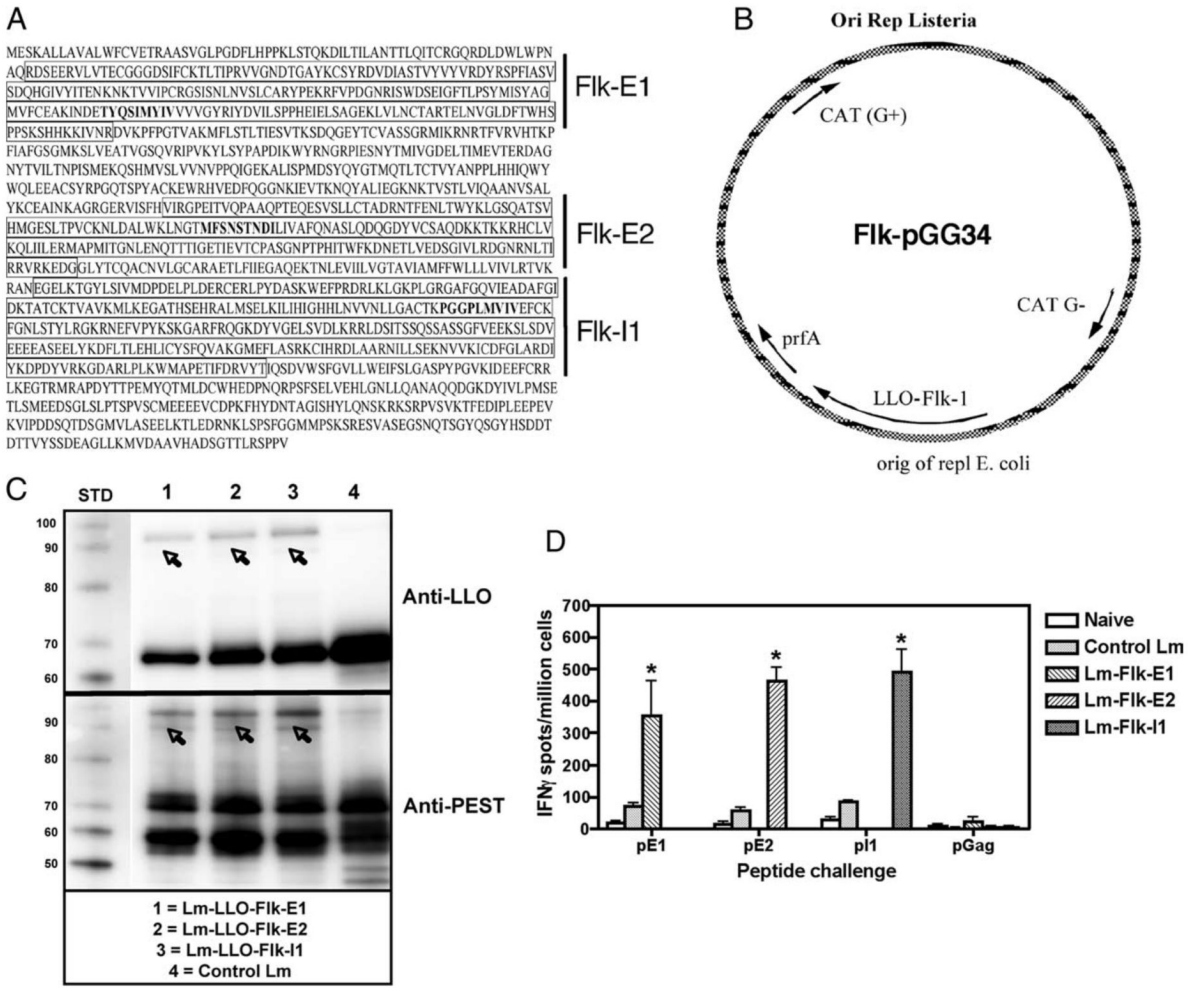

FIGURE 1.

Design of the Flk-1/VEGFR2-expressing *Lm*-based constructs. *A*, Cloned regions for each construct built are boxed; mapped CTL epitopes for the H-$2^{d/q}$ MHC I haplotype include the following: Flk_{210} (TYQSIMYIV), Flk_{613} (MFSNSTNDI), and Flk_{906} (PGGPLMVIV), and are shown in bold font (17). *B*, Each gene fragment was cloned into the expression vector pGG34 fused to LLO and placed under the control of the *hly* promoter. *C*, Western blot of proteins from culture supernatants showing expression of each fusion protein from the constructs listed. Polyclonal, rabbit, anti-PEST Ab was used for fusion protein detection (*bottom*), and mouse anti-LLO Ab was used for confirmation (*top*). Note that all lanes within a single blot were taken from the same Western blot; immunostaining was performed on two separate, but identical blots. *D*, IFN-γ ELISPOT showing $CD8^+$ T cell-restricted responses ex vivo after immunization with each construct. The naive group was injected with PBS alone; all groups contained a control *Lm* group. Responses are to the corresponding mapped epitopes for each Flk fragment, as follows: pE1 = Flk-$E1_{210–219}$ (TYQSIMYIV), pE2 = Flk-$E2_{613–622}$ (MFSNSTNDI), and pI1 = Flk-$I1_{906–915}$ (PGGPLMVIV); $n = 5$ per group. Graphs show mean ± SEM; *, $p < 0.05$; Mann-Whitney statistical test, experiment repeated once.

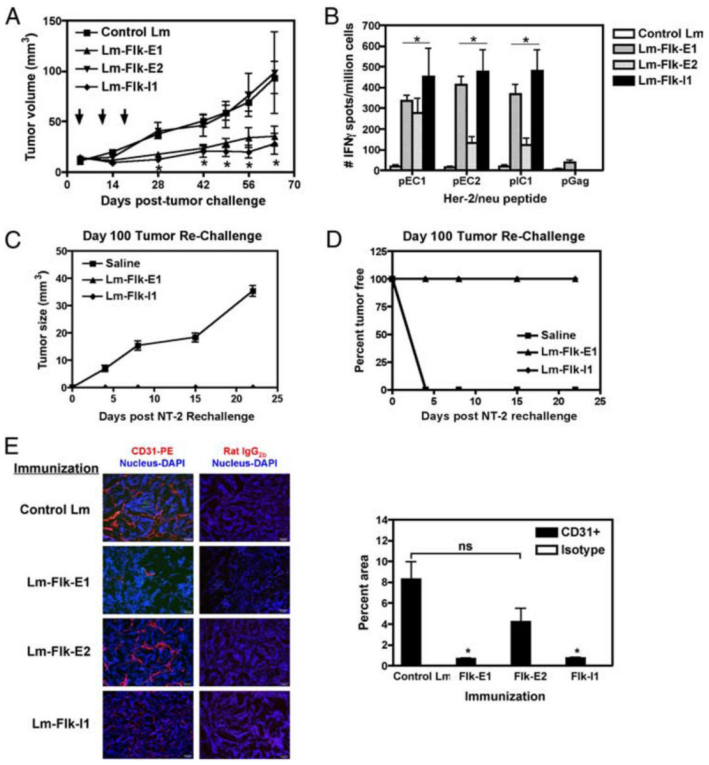

FIGURE 2.

Lm-LLO-Flk-1 vaccines can induce regression of established Her-2/*neu*$^+$ tumors in vivo. *A*, NT-2 tumor volume (mm^3) from mice treated with each construct. Graph shows mean ± SEM; *, $p < 0.05$; Mann-Whitney statistical test, $n = 8$ mice per group, experiment repeated twice. *B*, IFN-γ ELISPOTs showing epitope spreading to various Her-2/*neu* regions. Splenocytes from the 64-day time point were restimulated ex vivo with Her-2/*neu* peptide epitopes. Graph shows mean ± SEM; *, $p < 0.05$; Mann-Whitney statistical test, $n = 5$ mice per group, experiment repeated once. *C*, Mice that had fully regressed tumors were rechallenged with NT-2 in the contralateral flank on day 100. A saline-treated group was used as our negative control for tumor growth. *D*, Tumor volume for mice that grew tumors after rechallenge on day 100 of tumor-free mice. Both graphs refer to a single experiment. Number of tumor-free mice was two of eight for Flk-E1 and Flk-I1 groups; the saline group had five mice. *E*, Mice were immunized thrice over the course of 3 wk after the initial establishment of NT-2 tumors. In this figure (*right-hand panel*), we show staining for the pan-endothelial marker CD31-PE and nucleus using DAPI. Isotype controls were used on sequential sections, as shown to the *right*. Quantitation of vessel density, shown in the *left-hand panel*, was performed using Image Pro software. Graph shows mean ± SEM; *, $p < 0.05$; Mann-Whitney *U* test.

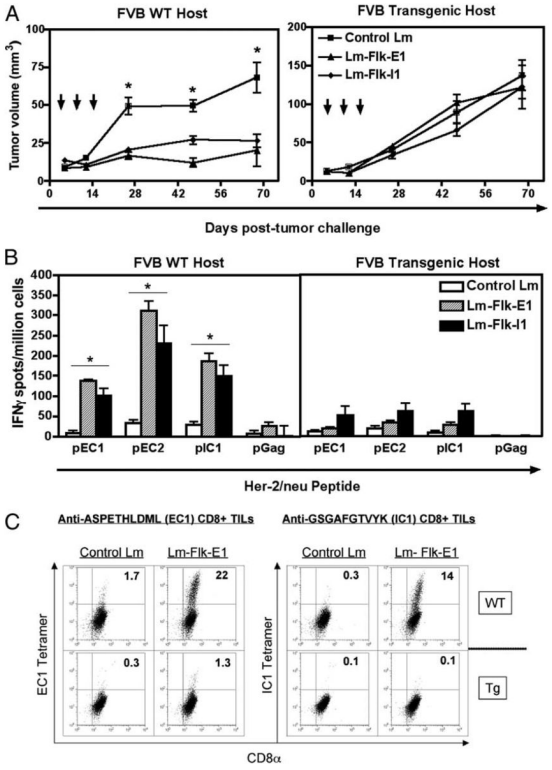

FIGURE 3.

Anti-angiogenesis vaccines are not effective in mice tolerant to HER-2/neu. *A*, FVB/N wild-type (WT) or FVB/N transgenic (Tg) mice were injected with 1×10^6 NT-2 cells s.c.; tumors were allowed to grow until palpable before treatment started. Mice were immunized a total of three times; mean tumor sizes are shown here for up to 69 days posttumor inoculation. Graphs show mean ± SEM; *, $p < 0.05$; Mann-Whitney *U* test, experiment repeated twice. *B*, Spleens were processed for IFN-γ ELISPOTs, and stimulated with various Her-2/neu peptides ex vivo, or a third-party peptide as a negative control (pGag). Graphs show mean ± SEM; *, $p < 0.05$; Mann-Whitney *U* test, experiment repeated once. *C*, Tumors from each group were pooled and digested for TILs; here we show Her-2/neu-specific T cells staining for CD8α and EC1- or IC1-specific tetramers. Significantly more Her-2/neu-specific T cells are found in the wild-type (WT), but not transgenic (Tg) mice; control *Lm* group shows low background. Experiment repeated once, giving similar results.

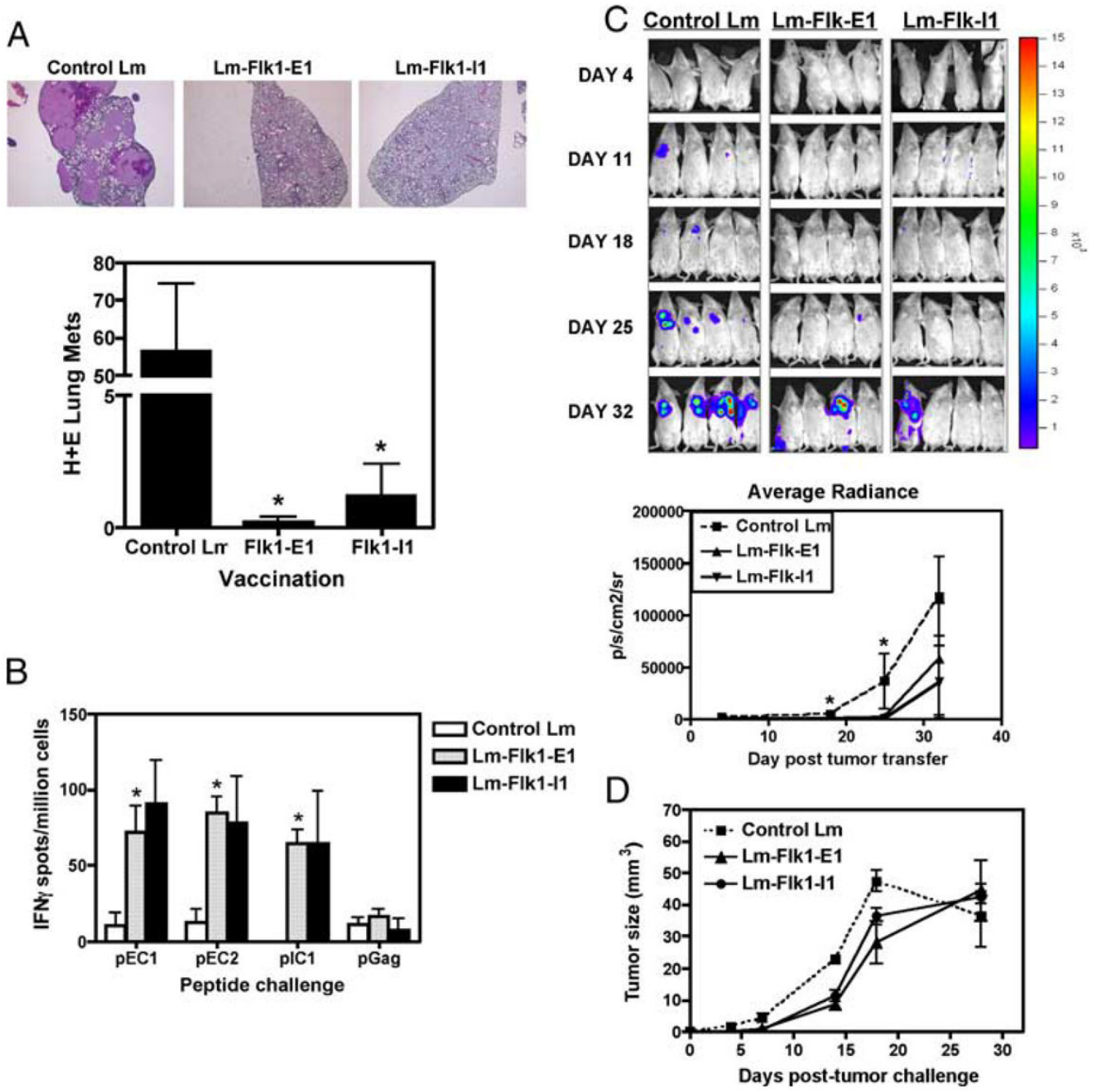

FIGURE 4.

Flk-1 vaccines can protect mice from experimental metastases and induce weak Her-2/neu epitope spreading in a more aggressive tumor model for breast cancer. *A*, Mice were immunized thrice with each vaccine, and then injected with 50,000 4T1 cells i.v.; tumors were allowed to grow for 25 days, and then mice were sacrificed. H&E-stained sections were performed on lung tissues, and tumor nodes were counted by hand. Graph shows the number of lung metastases per lobe per animal, mean ± SEM; *, $p < 0.05$; Mann-Whitney *U* test, experiment repeated once, $n = 5$ mice shown. *B*, Spleens from these animals were processed and rechallenged ex vivo in IFN-γ ELISPOT assays for Her-2/neu epitope spreading. The 4T1 cell line does express low levels of mouse Her-2/neu (48). Spreading is seen only in the Flk-1-E1-

immunized mice. Graph shows mean ± SEM for spot number/well as compared with control *Lm* group; *, $p < 0.05$; Mann-Whitney *U* test, experiment repeated once, $n = 5$ per group. *C*, A similar experiment in which mice were protected via immunization with each vaccine for a series of 3 wk, and then injected with 50,000 4T1-Luc cells i.v.; mice were imaged longitudinally over the course of 4 wk, looking for the incidence of lung seeding and rate of metastasis (*top panel*). Average radiance in photons (p) captured per second per cm^2 for the surface area (sr) gated in the region of interest is shown in the *bottom panel*. Graph shows mean ± SEM; *, $p < 0.05$; Mann-Whitney *U* test. Significance for mice is as follows: day 18, only Flk-E1 significant; day 25, both Flk-E1 and Flk-I1 significantly different when compared with control *Lm*. *D*, Primary s.c. 4T1 tumors grow more slowly in *Lm*-LLO-Flk-1-protected animals. Mice were immunized thrice with each vaccine, and then injected with s.c. and i.v. with 50,000 4T1 cells. Graph shows mean ± SEM for tumor volume.

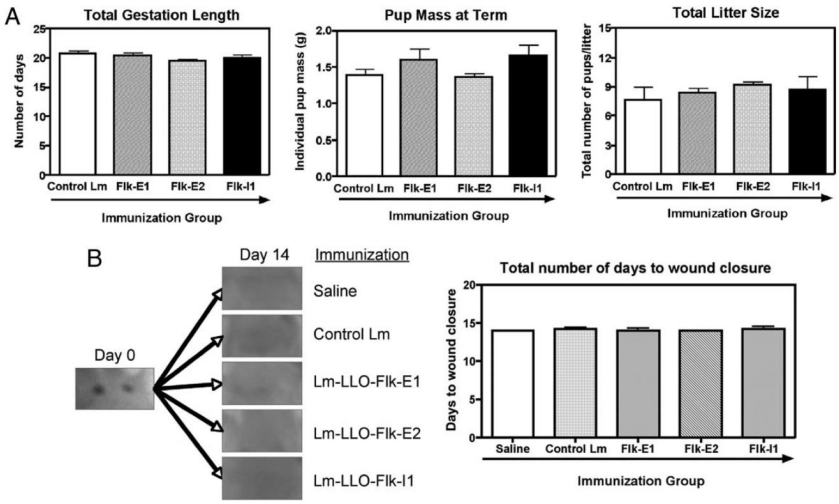

FIGURE 5.

Safety studies using the anti-angiogenesis Flk-1 vaccines. Mice were immunized thrice, as performed in all previous experiments, and then were allowed to either mate or entered into wound-healing studies. *A*, Mice (n = 5/group) were mated with syngeneic FVB/N males, and gestation was confirmed upon the observance of a vaginal plug following coitus. This was considered as day 0.5 days post-coitus. Total gestation length, pup mass at term, and total litter size were measured; graphs show mean ± SEM; *, $p < 0.05$. *B*, A pair of sterile skin biopsies was produced on the back of each vaccinated mouse (n = 5/group). Healing was observed on a daily basis. On day 14, healing was complete for all groups tested; near identical healing was observed for all groups. Graph shows the number of days until wound closure, mean ± SEM; *, $p < 0.05$; Mann-Whitney U test.

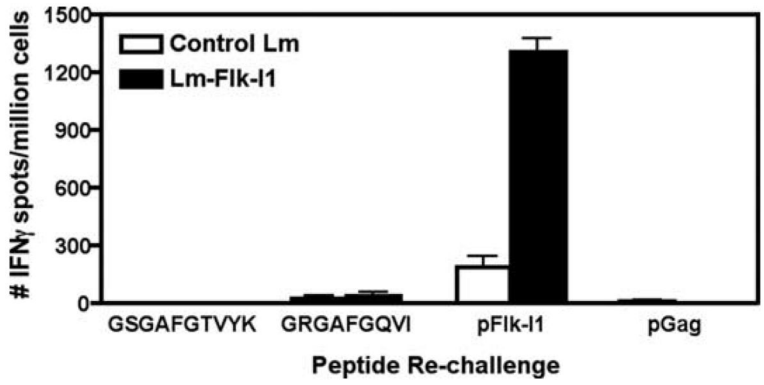

FIGURE 6.

Flk-1 vaccine-induced epitope spreading may not be due to cross-reactivity between Flk-1 and Her-2/neu shared domains. Mice were immunized thrice with either control *Lm* or Flk-I1 vaccine. Splenocytes were processed and rechallenged ex vivo for the secretion of IFN-γ in response to peptide challenge. Peptides included were the previously mapped pFlk-I1 epitope (PGGPLMVIV), a putative pIC1 epitope for Her-2/neu (GSGAFGTVYK) or the epitope in question, a putative shared epitope between the Her-2/neu and Flk-1 kinase domains (GRGAFGQVI), and a third-party epitope used as a negative control (pGag). Graph shows mean ± SEM; n = 3/group.